$\langle\overline{\psi}\psi\rangle$ at finite temperature with the overlap operator.

February 17, 2022

We used 10^4 perfectly decorrelated ($\tau = 0.5$) configurations to compute the eigenvalues. The chiral condensate is obtained through the following equations.

$$\Sigma = \frac{1}{V}\frac{\langle\det(D_m^{\text{ov}})^{N_f}\sum_\lambda \frac{1-\lambda/2}{(1-m/2)\lambda+m}\rangle}{\langle\det(D_m^{\text{ov}})^{N_f}\rangle}, \tag{1}$$

$$\det(D_m^{\text{ov}}) = \prod_\lambda \left[\left(1-\frac{m}{2}\right)\lambda + m\right]. \tag{2}$$

Since the eigenvalues come in complex pairs, the following versions of the determinant are valid as well

$$\det(D_m^{\text{ov}}) = \prod_{\lambda_1}\left|\left(1-\frac{m}{2}\right)\lambda_1 + m\right|^2 \prod_{\lambda_0}\left[\left(1-\frac{m}{2}\right)\lambda_0 + m\right], \tag{3}$$

$$\det(D_m^{\text{ov}}) = \prod_{\lambda_2}\left|\left(1-\frac{m}{2}\right)\lambda_2 + m\right|^2 \prod_{\lambda_0}\left[\left(1-\frac{m}{2}\right)\lambda_0 + m\right], \tag{4}$$

where

$$\lambda_0 \in \{\lambda\,|\,\text{Im}(\lambda) = 0\}, \quad \lambda_1 \in \{\lambda\,|\,\text{Im}(\lambda) > 0\}, \quad \lambda_2 \in \{\lambda\,|\,\text{Im}(\lambda) < 0\}. \tag{5}$$

To calculate the determinant without losing precision, we take its logarithm and determine the sum

$$\sum_{\lambda_1}\log\left|\left(1-\frac{m}{2}\right)\lambda_1 + m\right|^2 + \sum_{\lambda_0}\log\left[\left(1-\frac{m}{2}\right)\lambda_0 + m\right]. \tag{6}$$
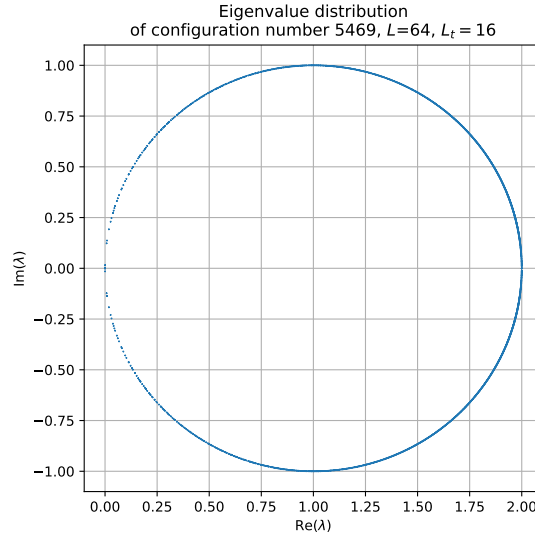
After exponentiation we obtain $\det(D_m^{\text{ov}})$.
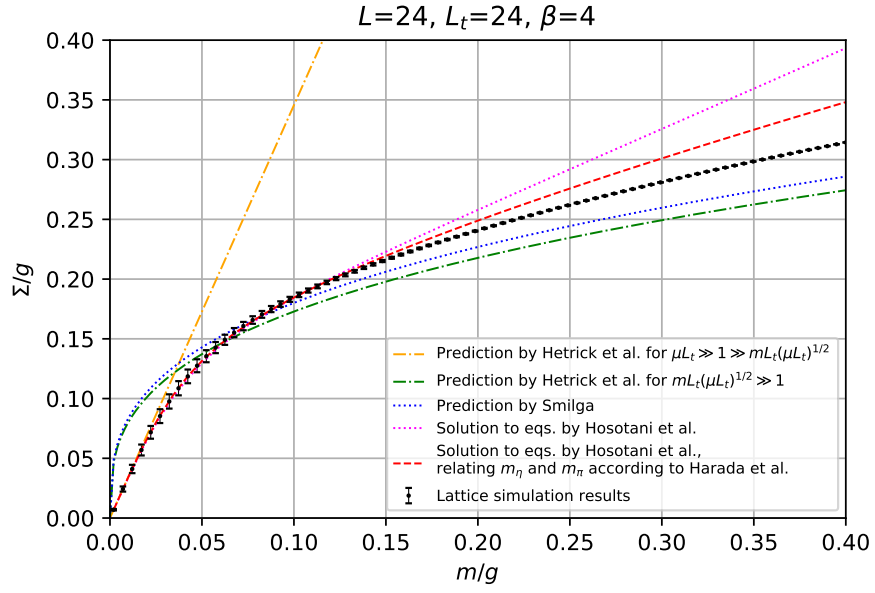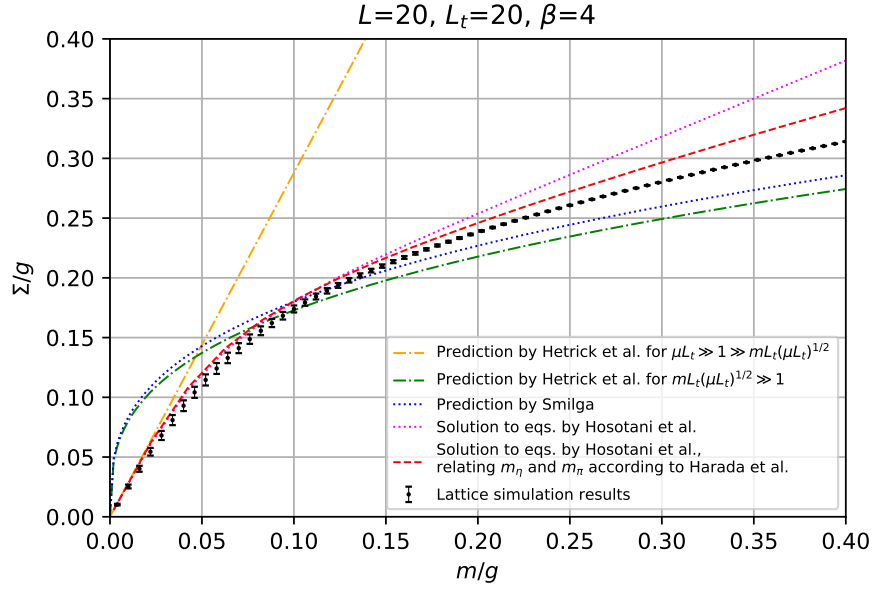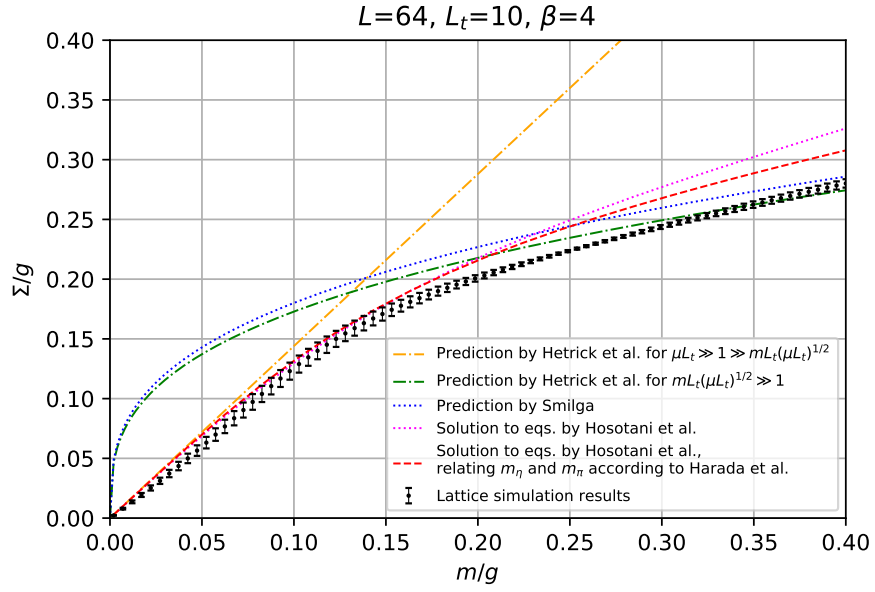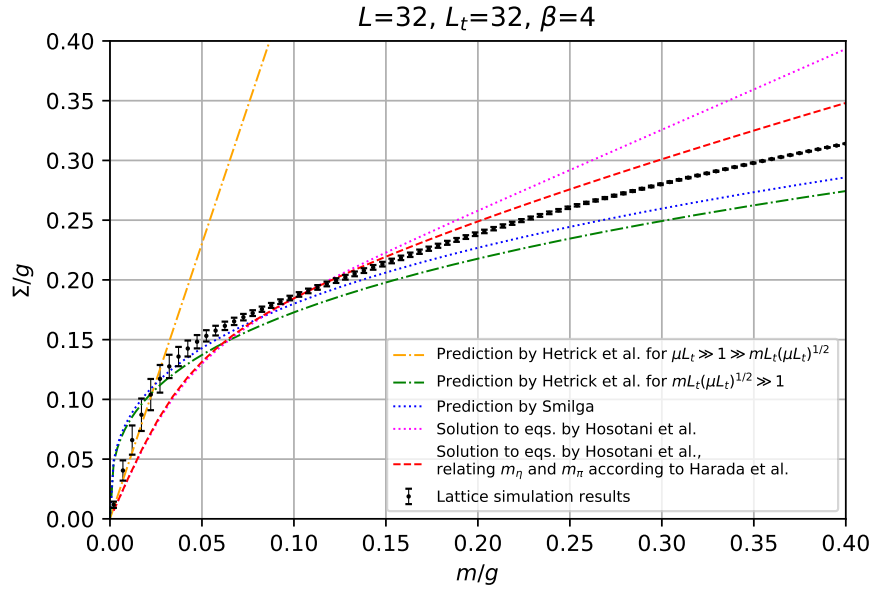

Figure 1: Typical eigenvalue distribution.

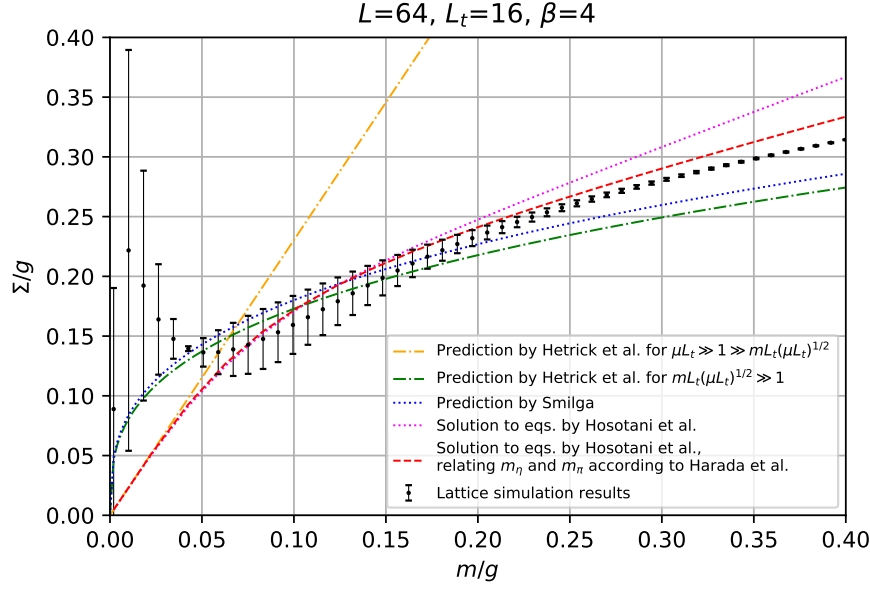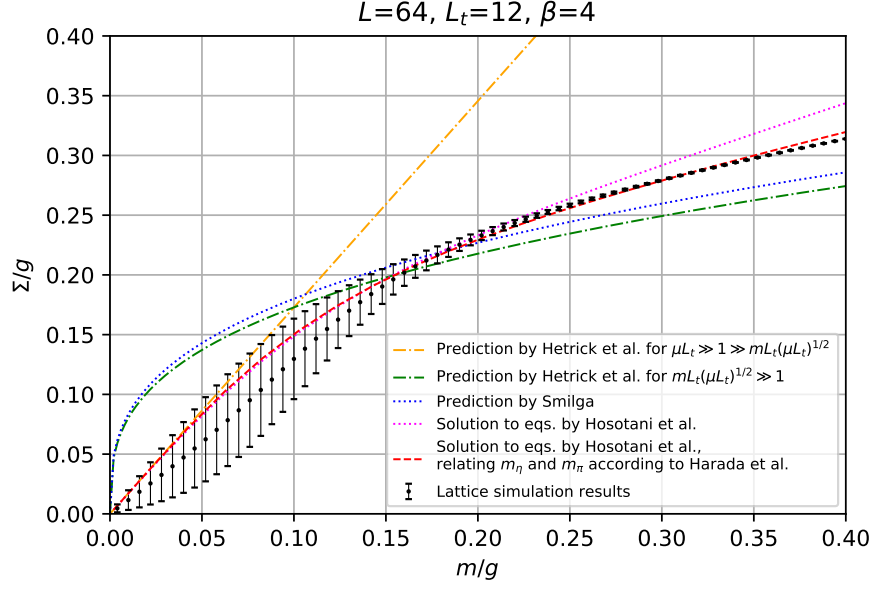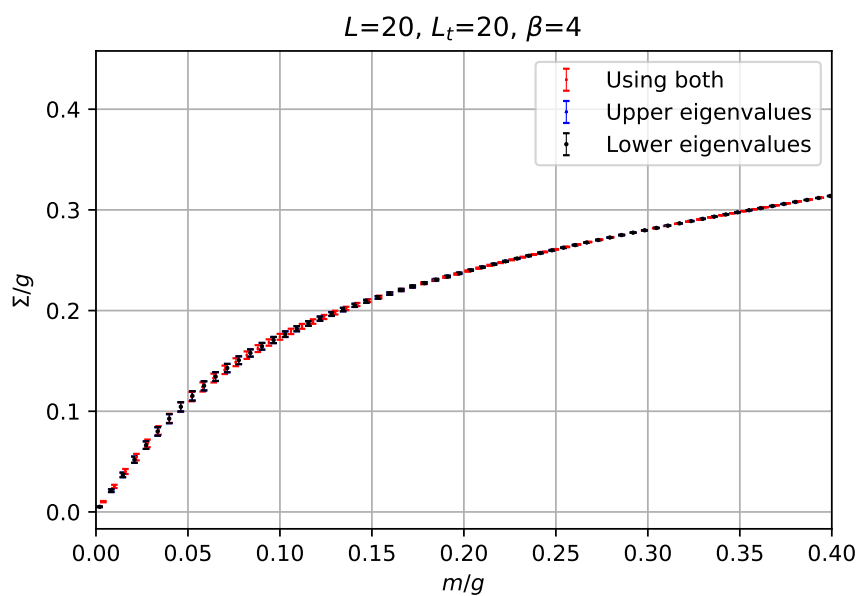# 1   Lattice vs. Hosotani's equations

(a) $\langle \overline{\psi}\psi \rangle$ for a lattice of size 20x20.

(b) $\langle \overline{\psi}\psi \rangle$ for a lattice of size 24x24.

(c) $\langle \overline{\psi}\psi \rangle$ for a lattice of size 32x32.

(d) $\langle \overline{\psi}\psi \rangle$ for a lattice of size 64x10.

(e) $\langle \overline{\psi}\psi \rangle$ for a lattice of size 64x12.

(f) $\langle \overline{\psi}\psi \rangle$ for a lattice of size 64x16.

Figure 2: Chiral condensate for different lattices.

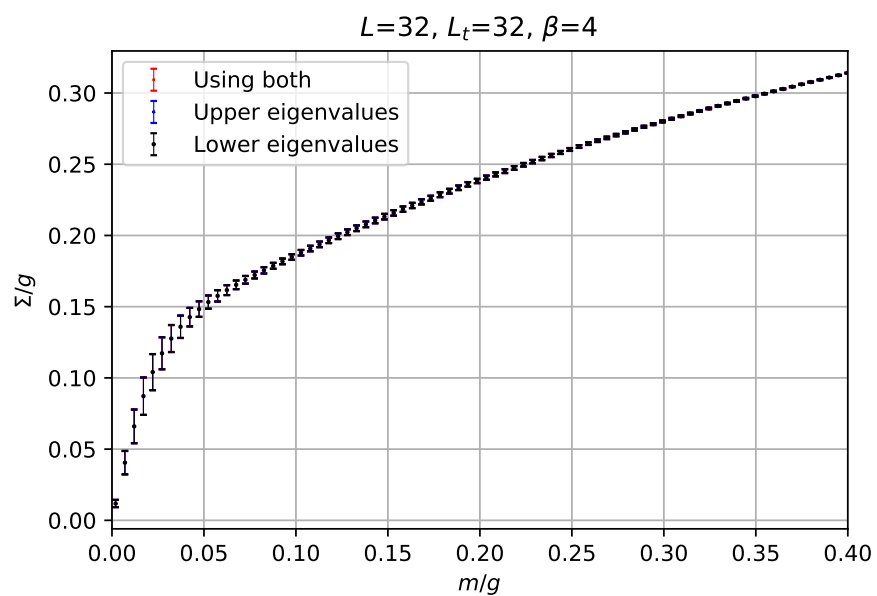# 2 Comparison of Σ with the lower and upper half plane eigenvalues.

The calculation of the determinant (2) can be done by using only the zero modes and either the eigenvalues with $\text{Im}(\lambda) > 0$ or $\text{Im}(\lambda) < 0$, since they come in complex pairs. We compare the outcome of both approaches, together with the result of using all the eigenvalues.
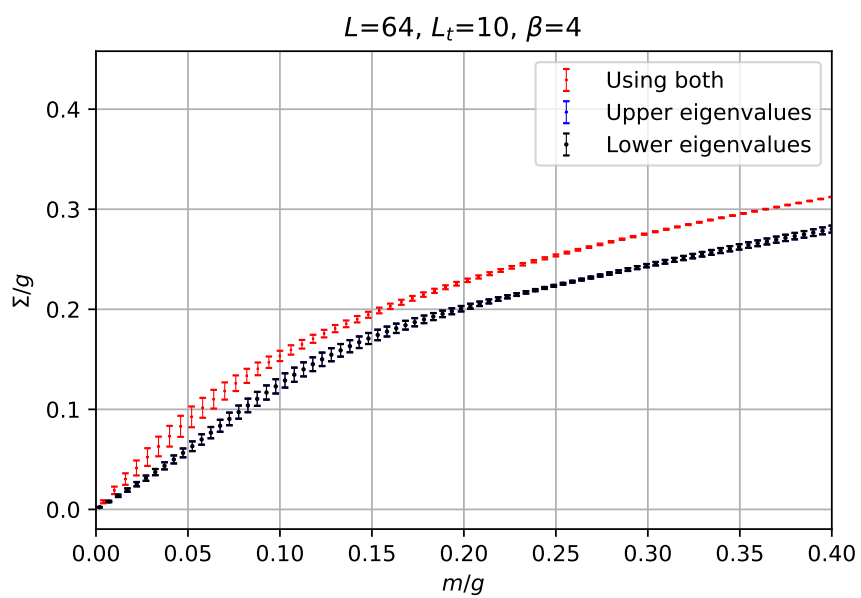
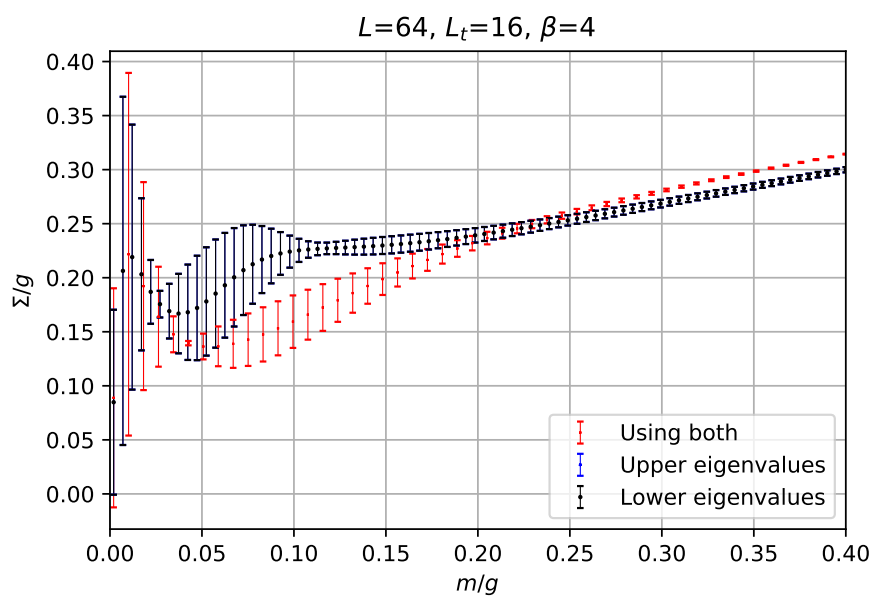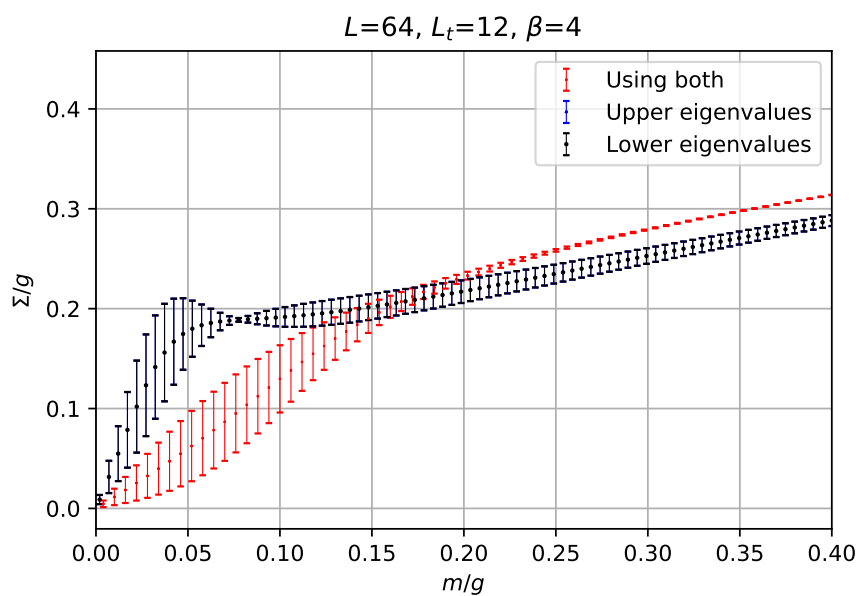(a) $\langle \overline{\psi}\psi \rangle$ for a lattice of size 20x20.
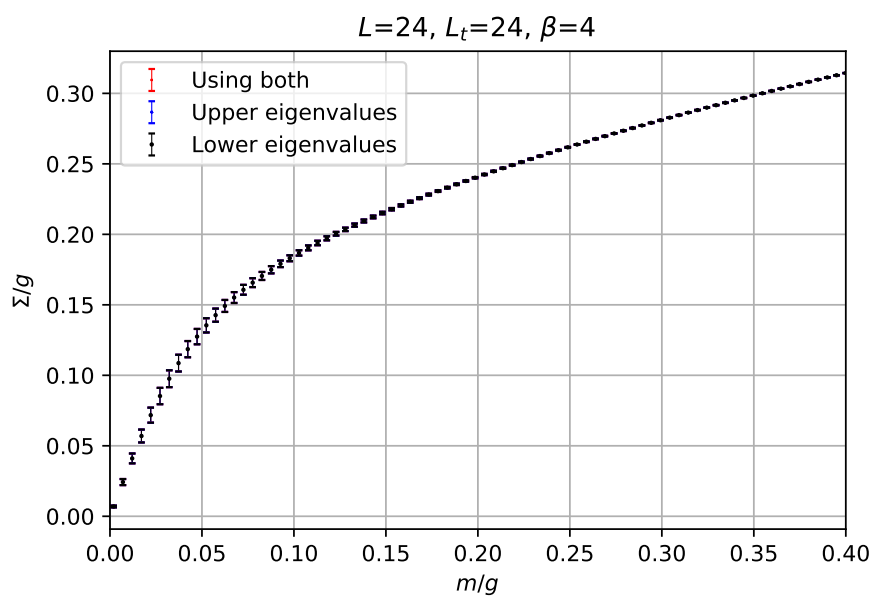
(b) $\langle \overline{\psi}\psi \rangle$ for a lattice of size 24x24.

(c) $\langle \overline{\psi}\psi \rangle$ for a lattice of size 32x32.

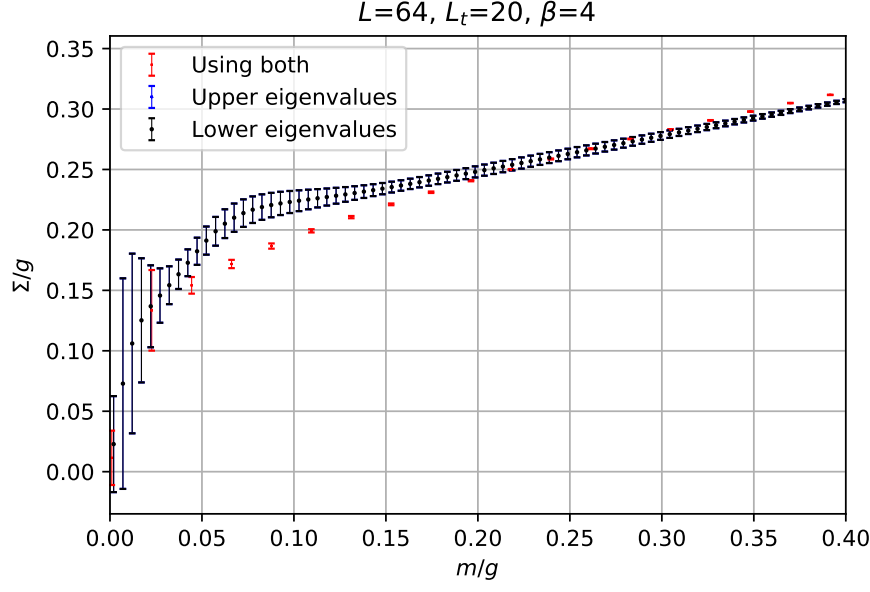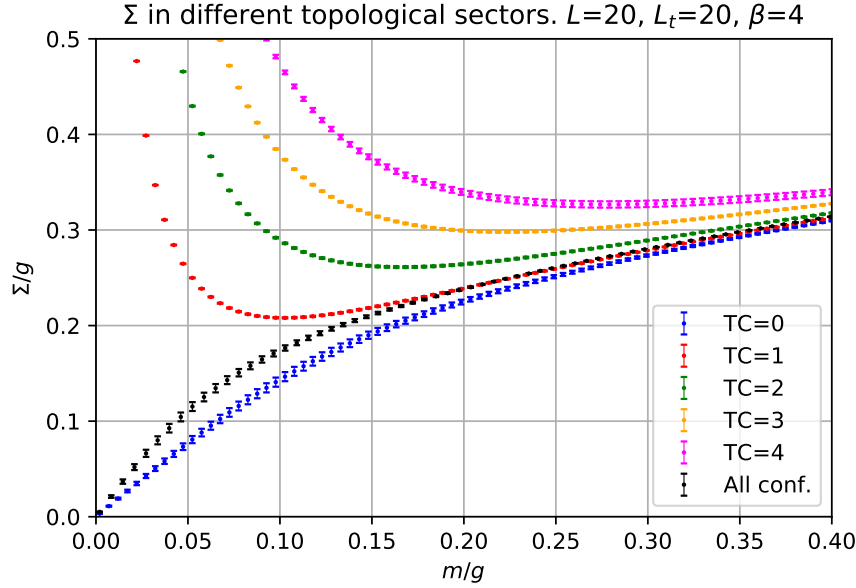(d) $\langle \overline{\psi}\psi \rangle$ for a lattice of size 64x10.

(e) $\langle \overline{\psi}\psi \rangle$ for a lattice of size 64x12.

(f) $\langle \overline{\psi}\psi \rangle$ for a lattice of size 64x16.

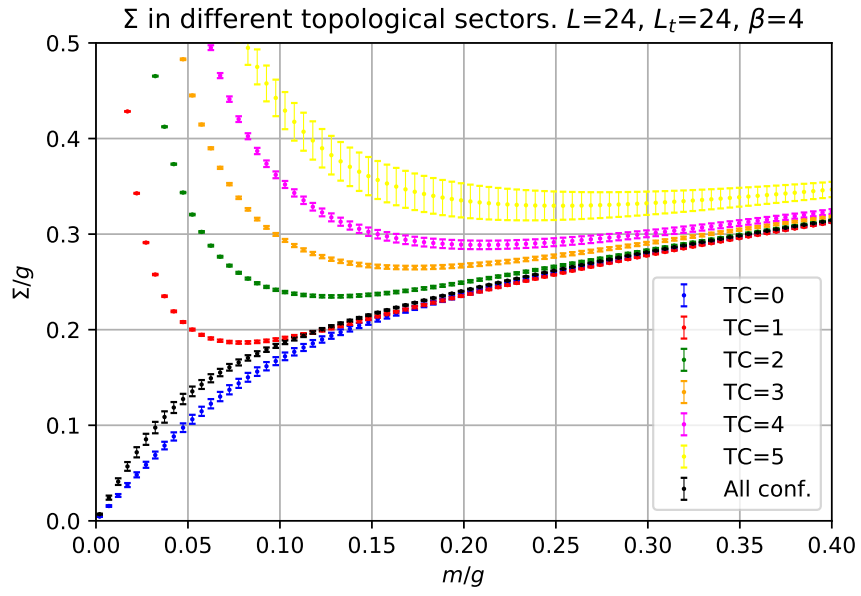(g) $\langle \overline{\psi}\psi \rangle$ for a lattice of size 64x20.

Figure 3: The blue points were computed by using only the eigenvalues which satisfy $\text{Im}(\lambda) > 0$ and the zero modes. In a similar way, the black points were computed by using those eigenvalues with $\text{Im}(\lambda) < 0$ and the zero modes. The red points are the results when we consider both regions of the complex plane to compute the determinant of the overlap operator.
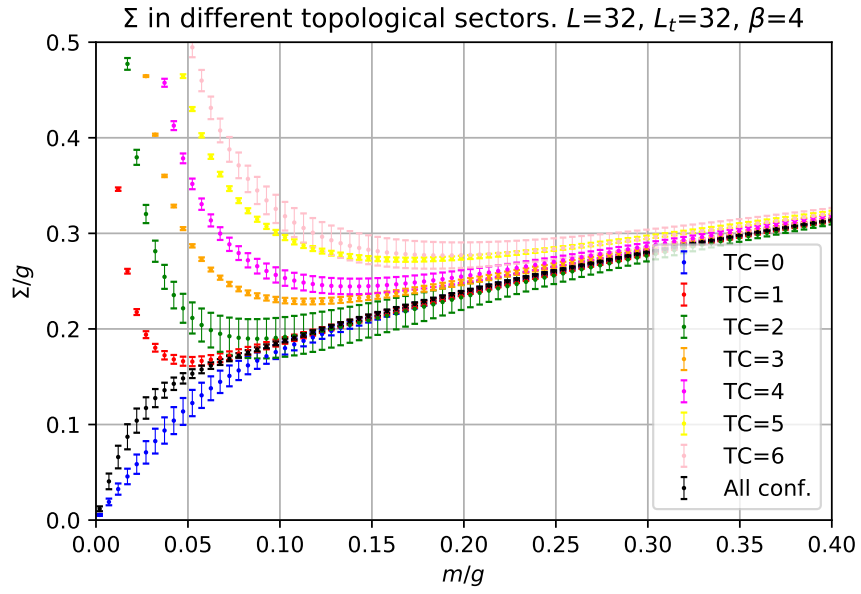
3 Σ in different topological sectors

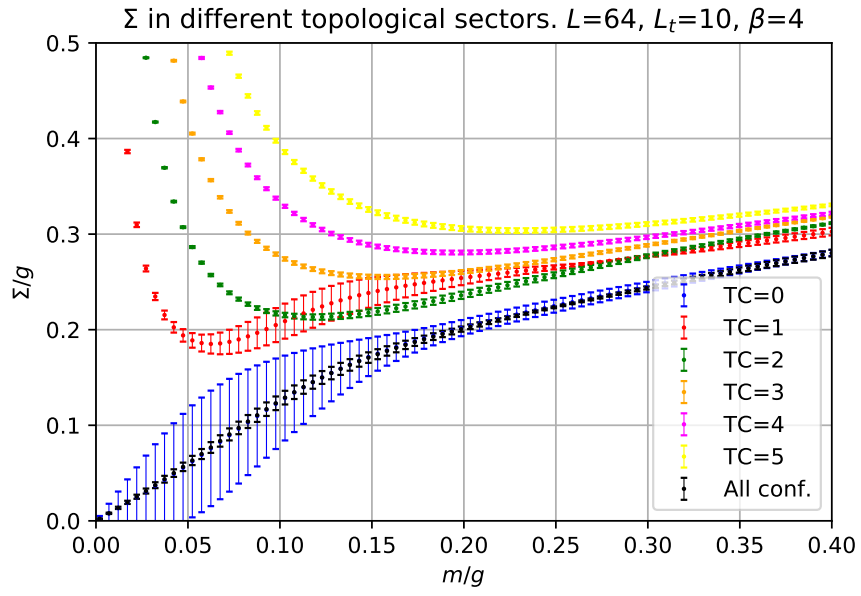We present the values of Σ in different topological sectors.

(a) $\langle \overline{\psi}\psi \rangle$ for a lattice of size 20x20.
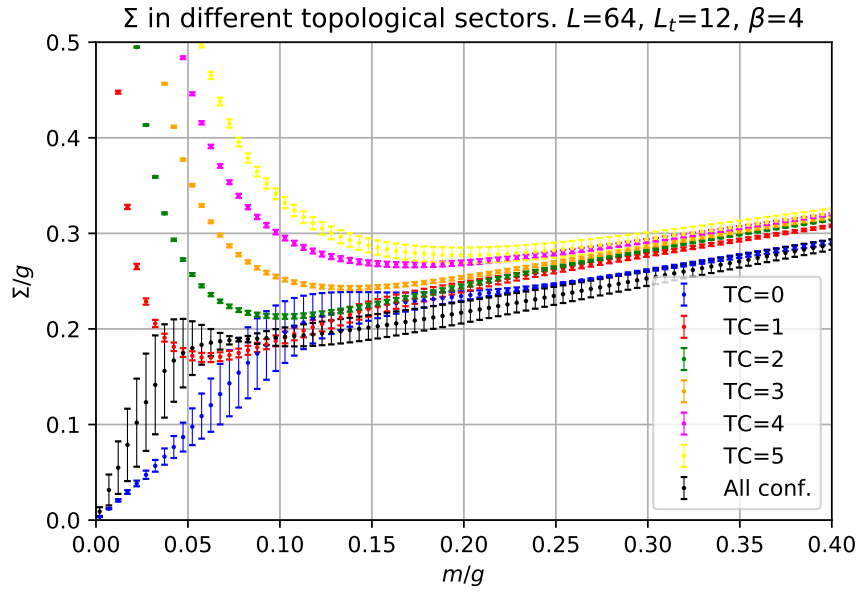
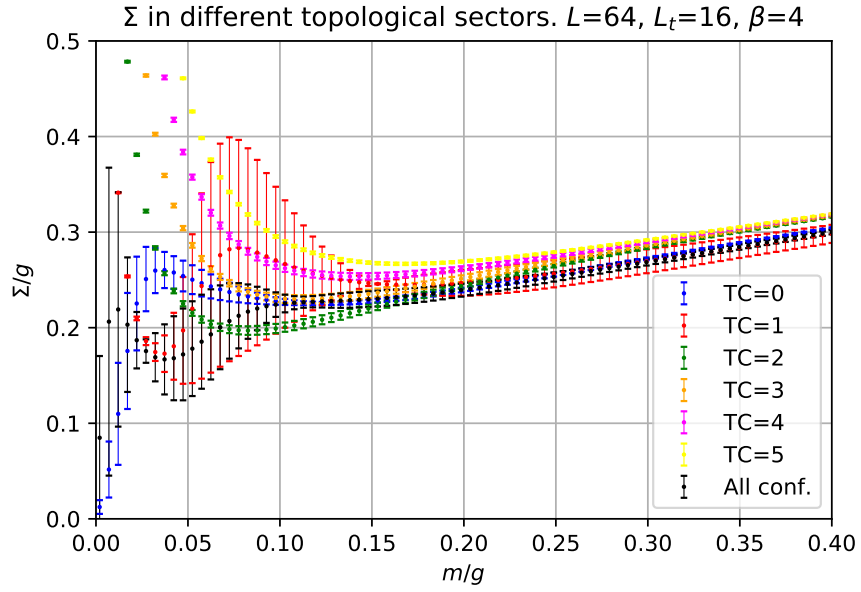(b) $\langle \overline{\psi}\psi \rangle$ for a lattice of size 24x24.

(c) $\langle \overline{\psi}\psi \rangle$ for a lattice of size 32x32.
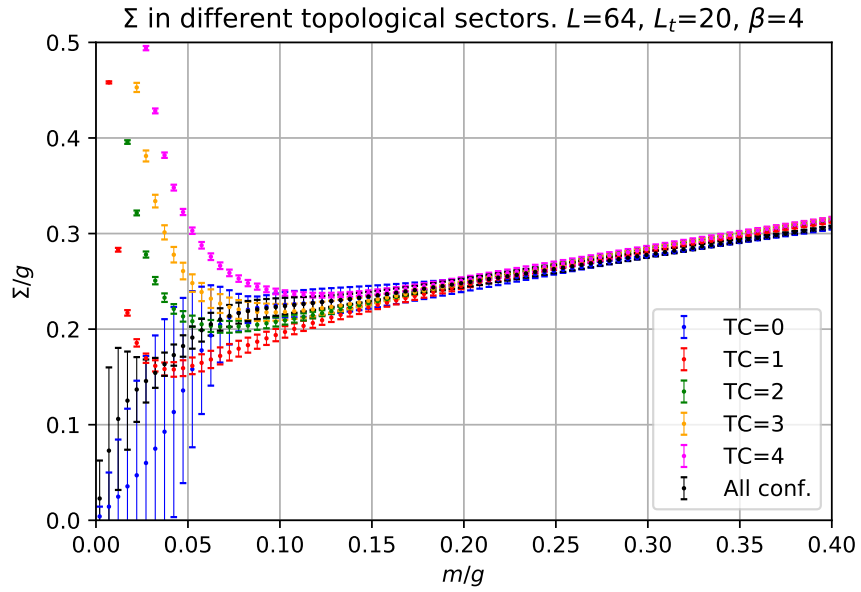
(d) $\langle \overline{\psi}\psi \rangle$ for a lattice of size 64x10.

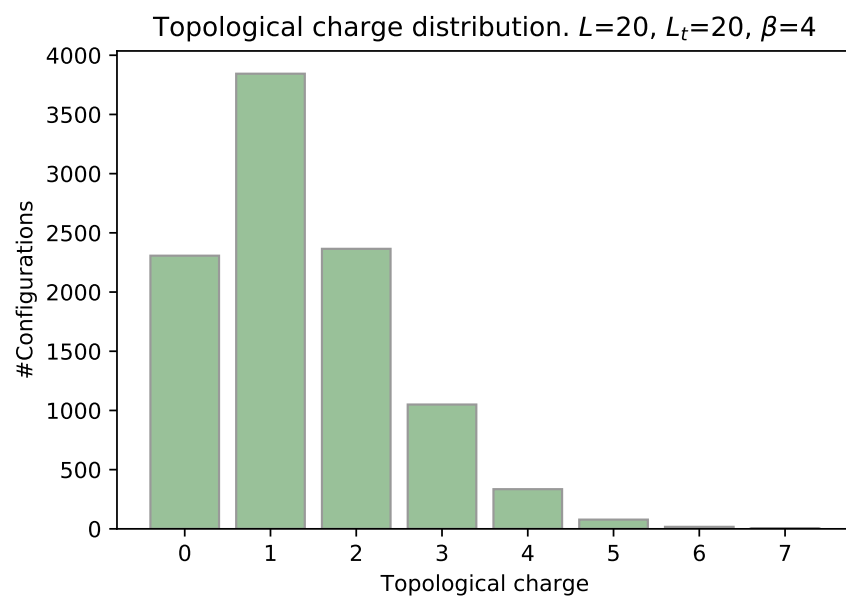(e) $\langle \overline{\psi}\psi \rangle$ for a lattice of size 64x12.

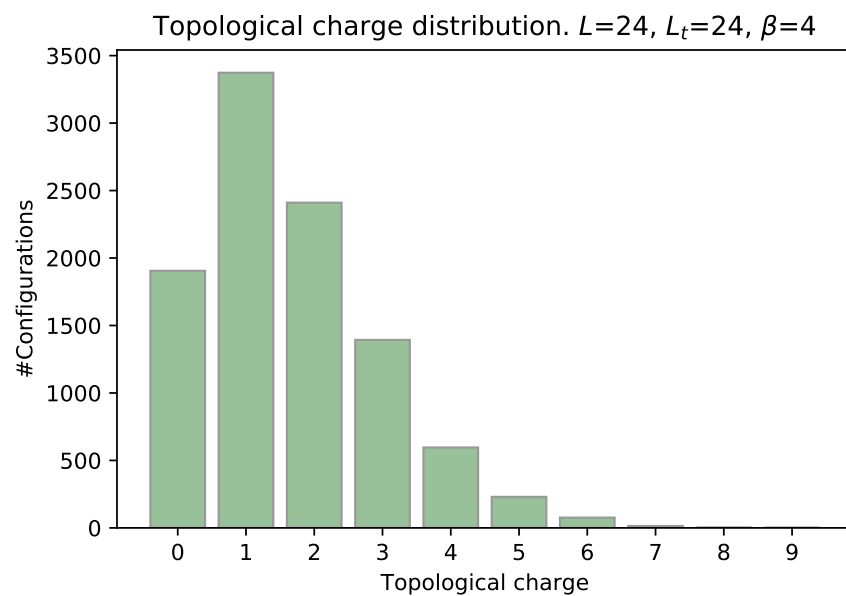(f) $\langle \overline{\psi}\psi \rangle$ for a lattice of size 64x16.

(g) $\langle \overline{\psi}\psi \rangle$ for a lattice of size 64x20.

Figure 4: We compute Σ in each topological sector, labeled by TC, by using only those configurations with topological charge TC and applying formula (1).
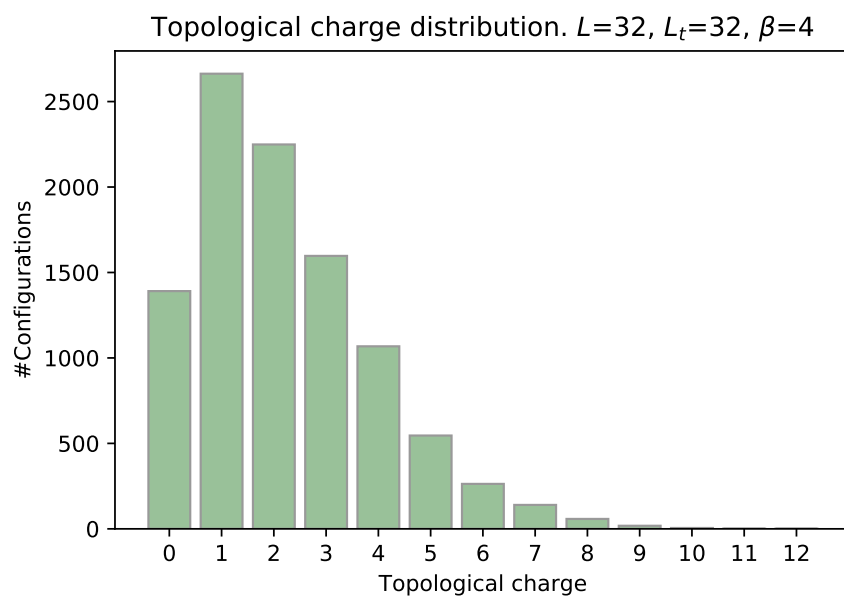
In the following figure we show the distribution of the topological charge.
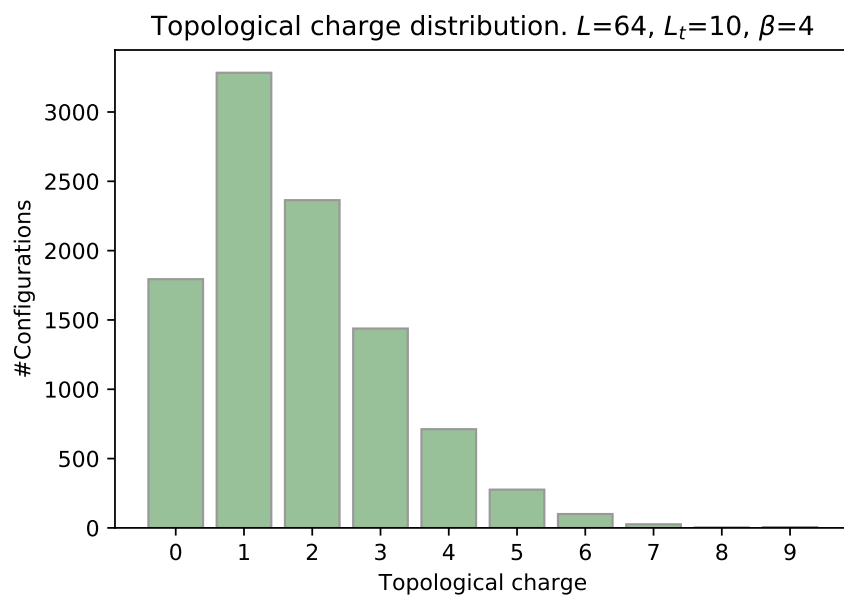
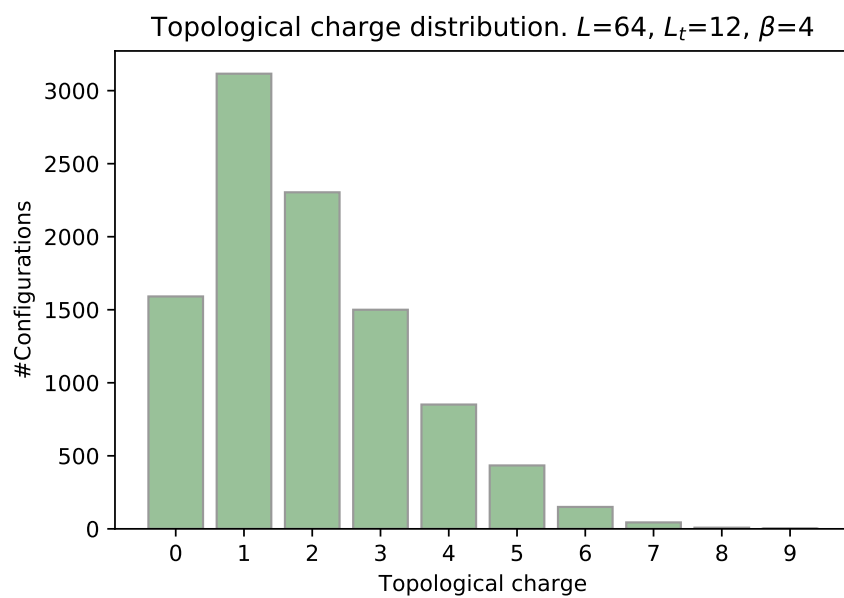(a) Distribution of topological charge for a lattice of size 20x20.

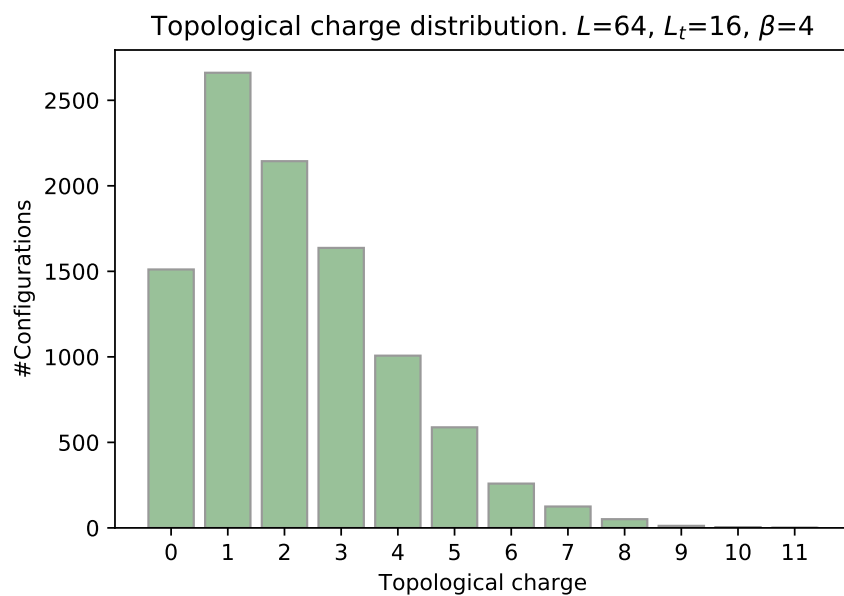(b) Distribution of topological charge for a lattice of size 24x24.

Topological charge distribution. L=32, L_t=32, β=4

(c) Distribution of topological charge for a lattice of size 32x32.

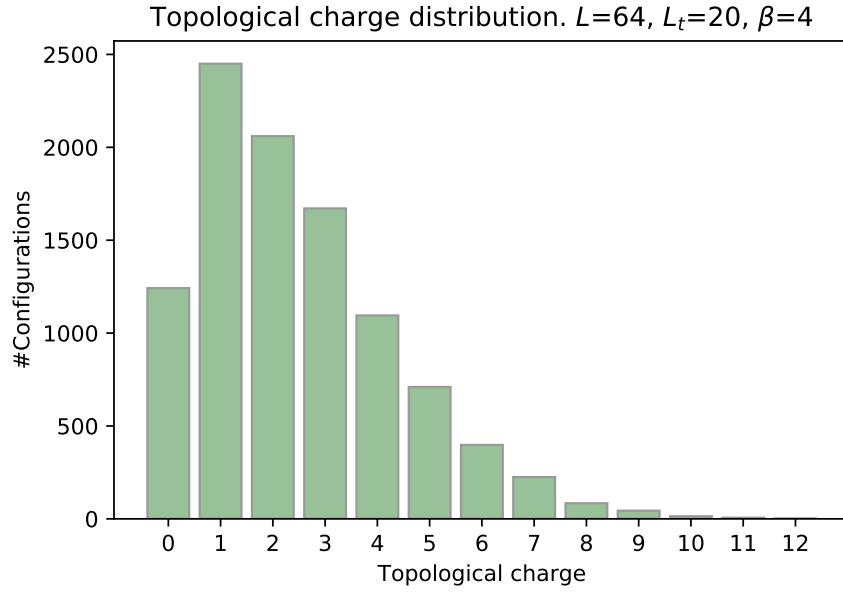Topological charge distribution. L=64, L_t=10, β=4

(d) Distribution of topological charge for a lattice of size 64x10.

(e) Distribution of topological charge for a lattice of size 64x12.

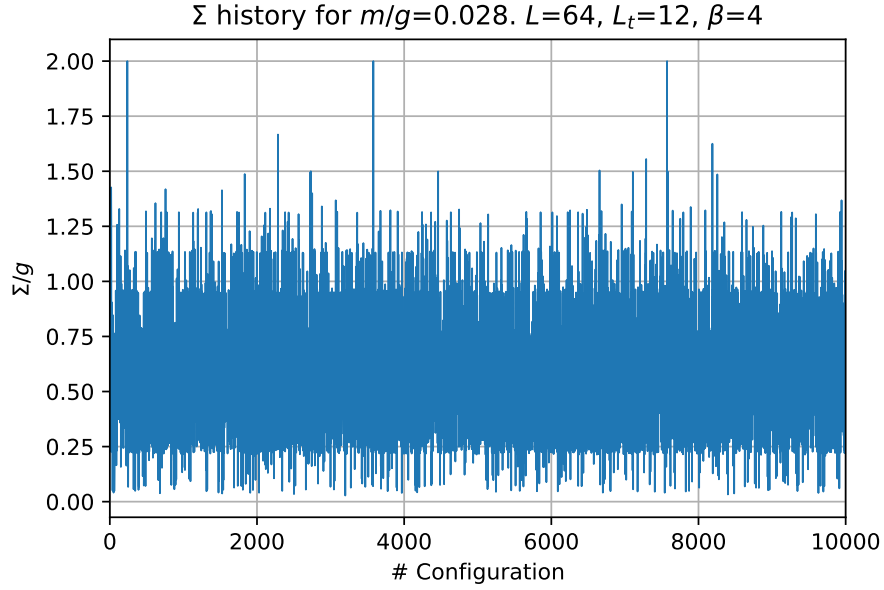(f) Distribution of topological charge for a lattice of size 64x16.

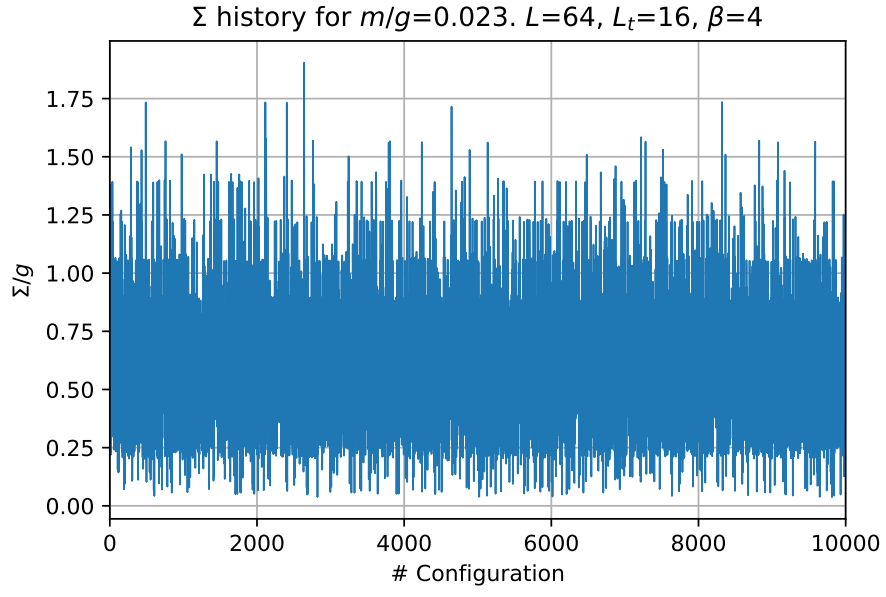(g) Distribution of topological charge for a lattice of size 64x20.

Figure 5: Distribution of the topological charge for different lattices.

4 Σ "History" (Σ vs. Conf. Number)

We show Σ as a function of the configuration number for different masses and different lattices.

(a)

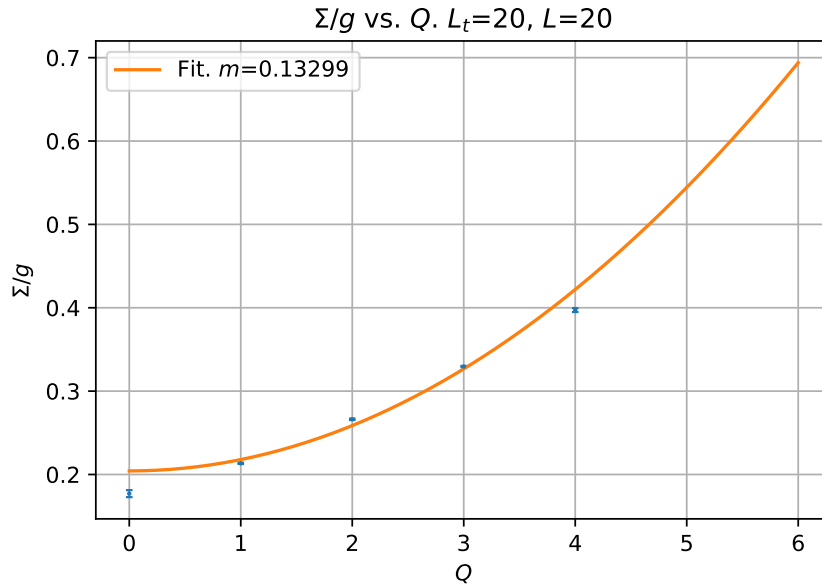Figure 6: Σ history for different lattices and masses.

5   Fits
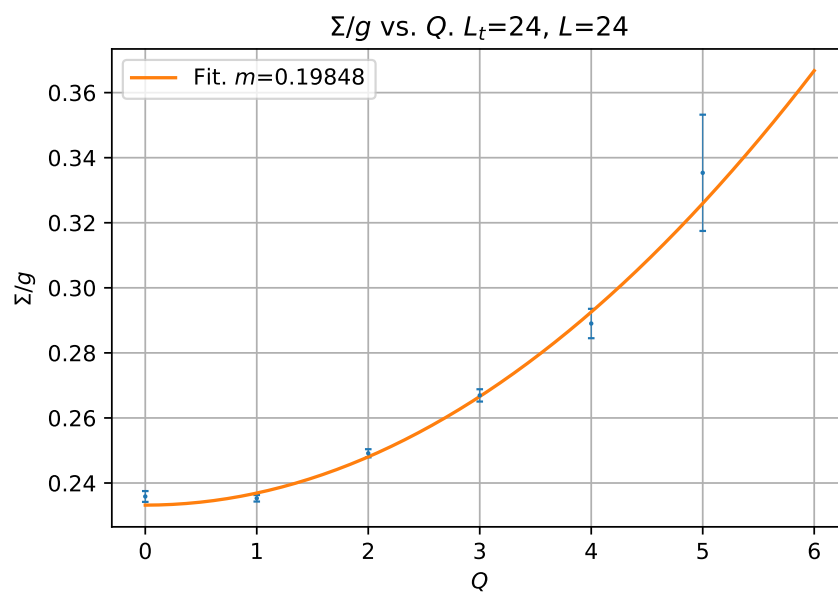
We fitted a function of the form

$$\frac{\Sigma}{g}(Q) = \frac{\Sigma_0}{g} + \frac{c}{LL_t\chi_t}\left(1 - \frac{Q^2}{LL_t\chi_t}\right) \tag{7}$$

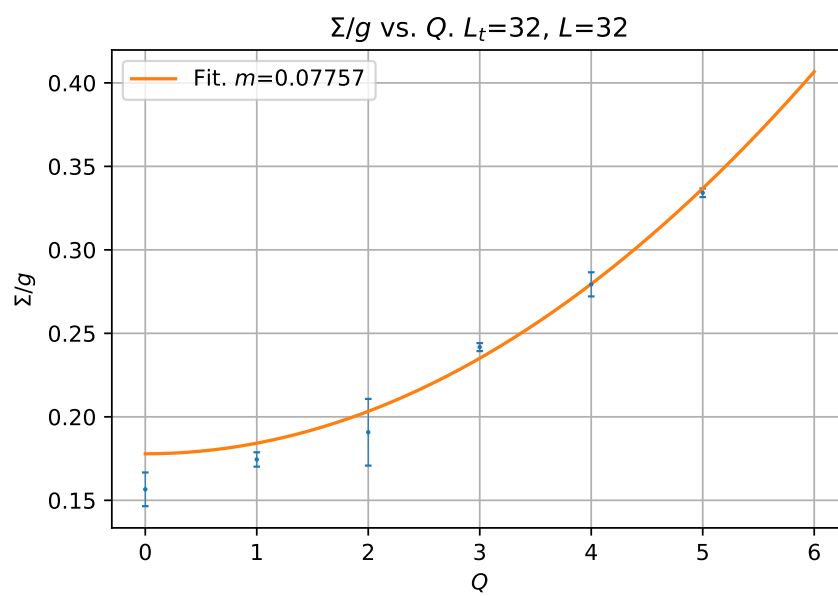to the data set Σ/g vs. Q, where Q denotes the topological charge, for specific masses.
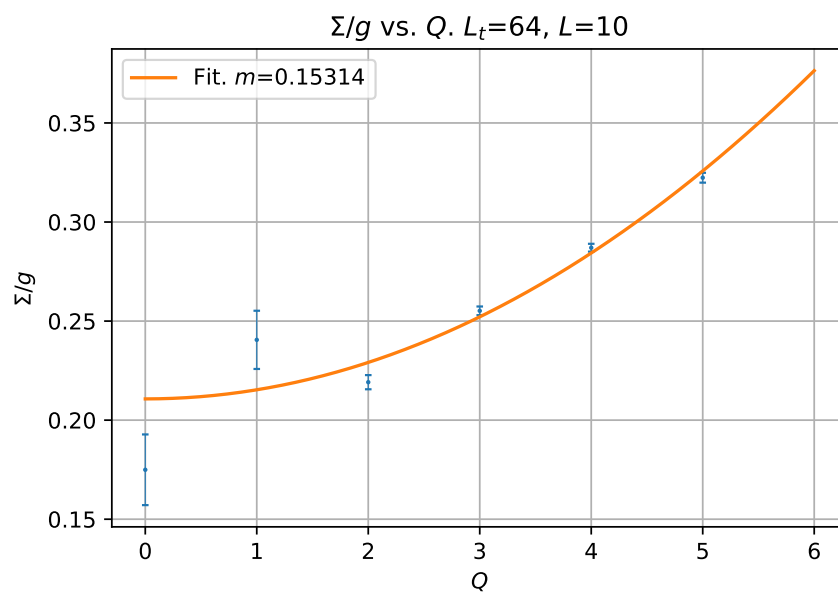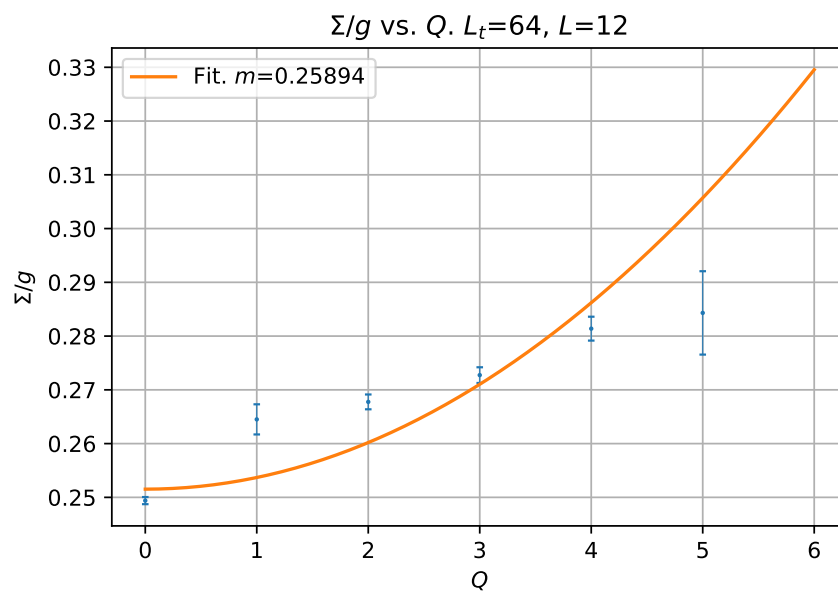
Σ/g vs. Q. L_t=24, L=24

Fit. m=0.19848

(b)

Σ/g vs. Q. L_t=32, L=32

Fit. m=0.07757

(c)

Σ/g vs. Q. L_t=64, L=10

Fit. m=0.15314

(d)

Σ/g vs. Q. L_t=64, L=12

Fit. m=0.25894

(e)

Σ/g vs. Q. L_t=64, L=16

Fit. m=0.34458
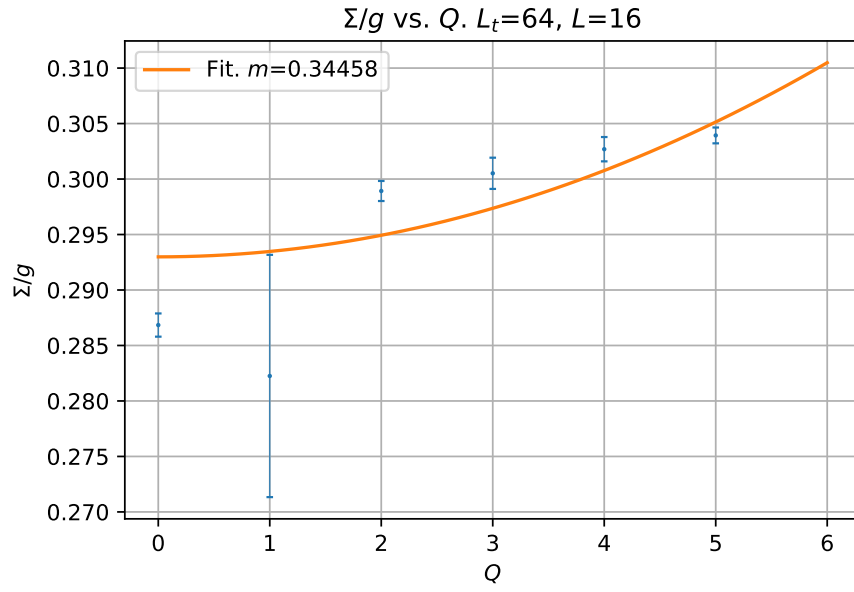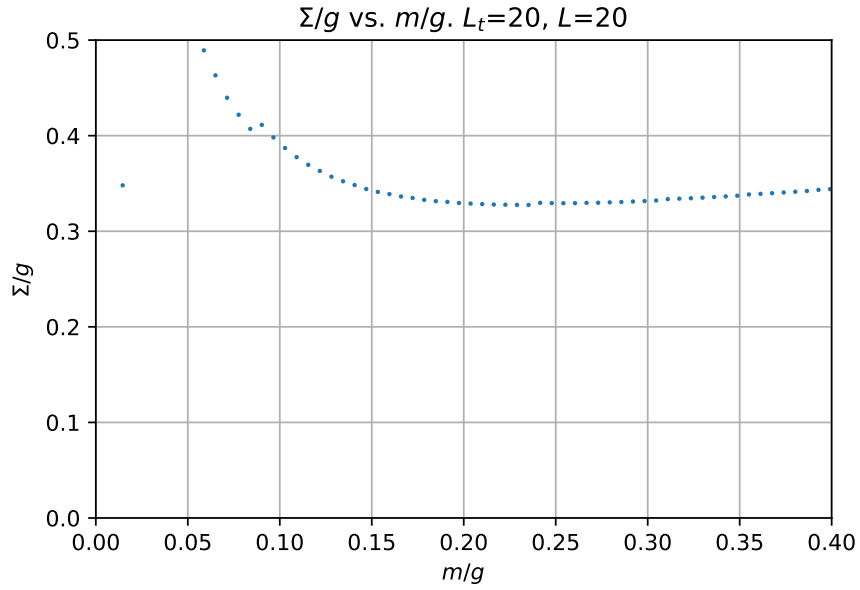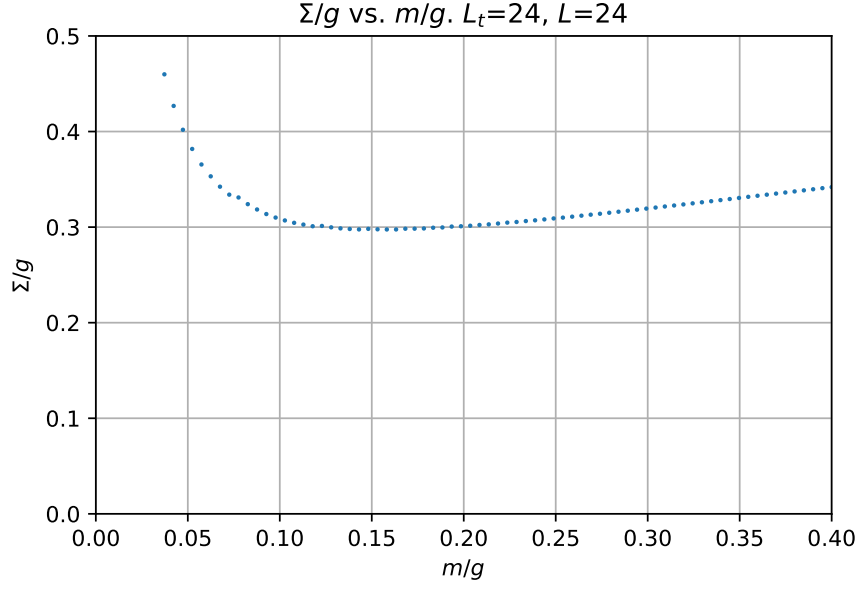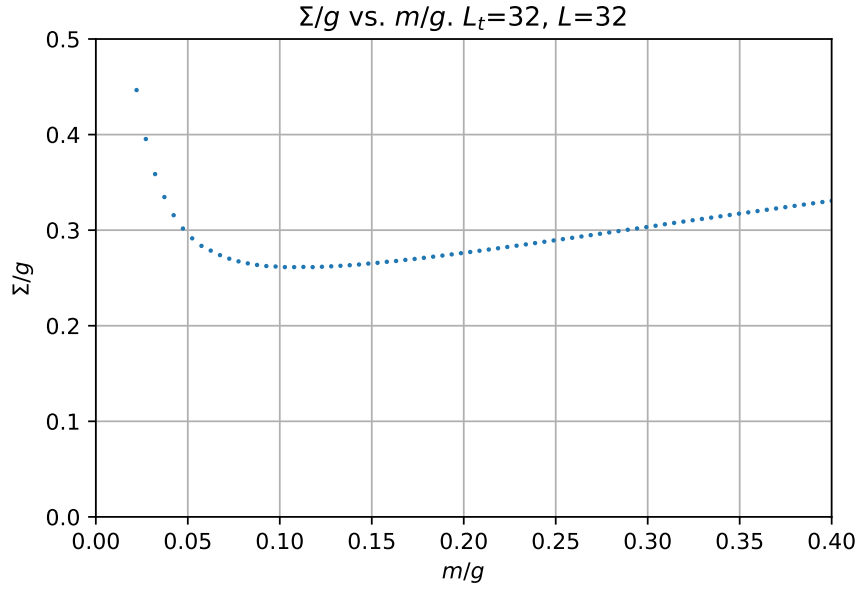
(f)

Figure 7: Fits

We performed this same procedure to all the masses of the square lattices. This allows to plot Σ as a function of the mass for $N_f = 0$.


Σ/g vs. m/g. L_t=20, L=20

(a)

(b)

(c)

Figure 8: Chiral condensate obtain through the fit of eq. (7).

6 Determinant vs. smallest eigenvalue (not zero mode)

In order to understand the behavior of the chiral condensate on the non-square lattices, we select those configurations where the value of Σ is different when we calculate it using only half of the eigenvalues and using all of them. Then, we plot the determinant shown in eq. (2) vs. $\min[|\text{Im}(\lambda)| : \text{Im}(\lambda) \neq 0]$.

Determinant vs. smallest Im(λ). L_t=64, L=10

(a)

Determinant vs. smallest Im(λ). L_t=64, L=12
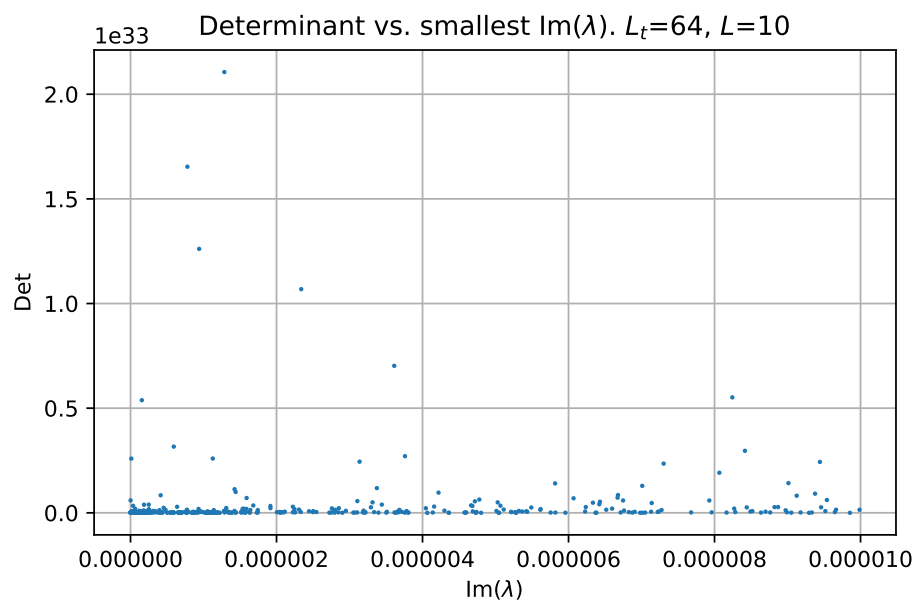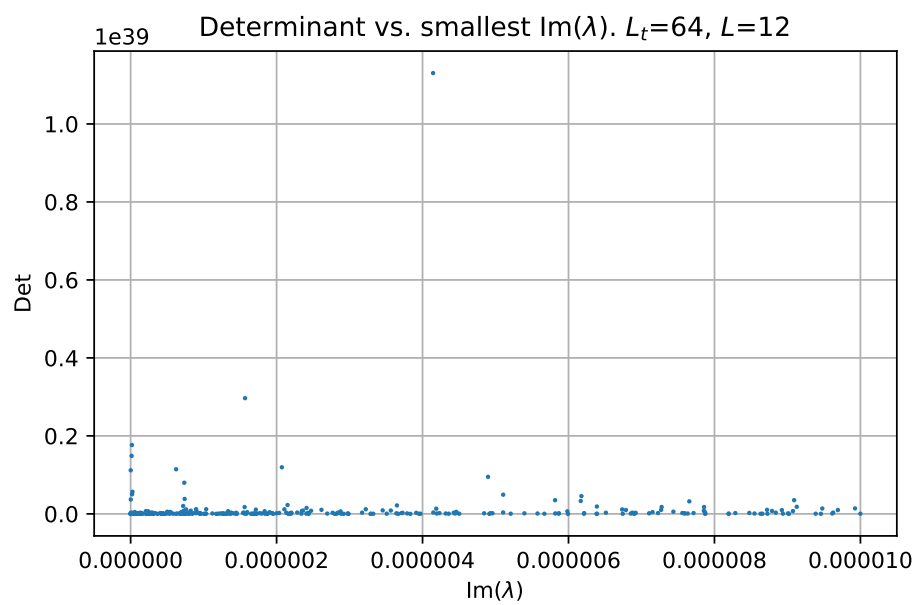
(b)
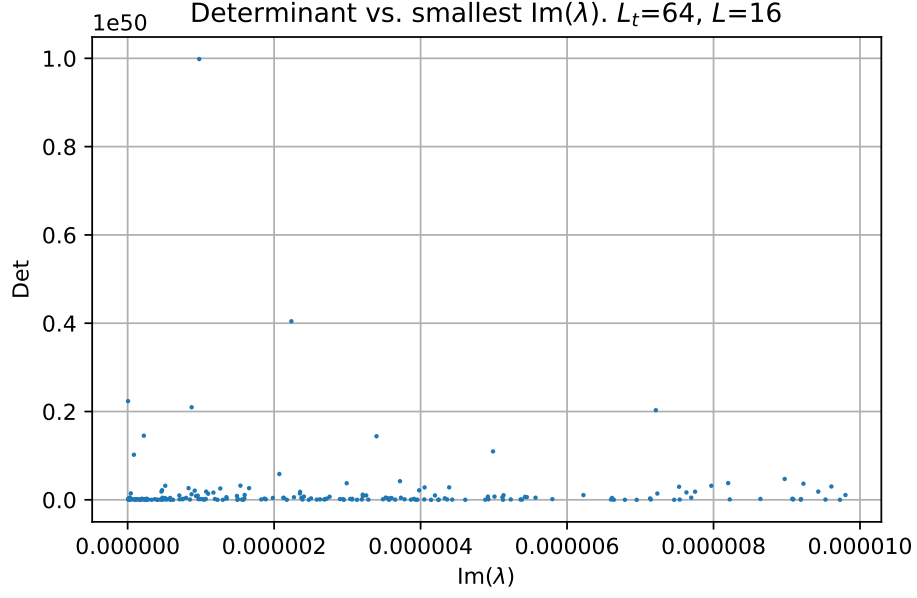
(c)

Figure 9: We observe that all the *ill* configurations have an eigenvalue with imaginary part smaller than 1×10^{-5} and larger or equal than 1×10^{-10}. The zero modes have imaginary part $\sim 1 \times 10^{-15}$.

We also show the topological charge distribution of the ill configurations.

(a)

Topological charge distribution of ill configurations.
$L=64$, $L_t=12$, $\beta=4$

(b)

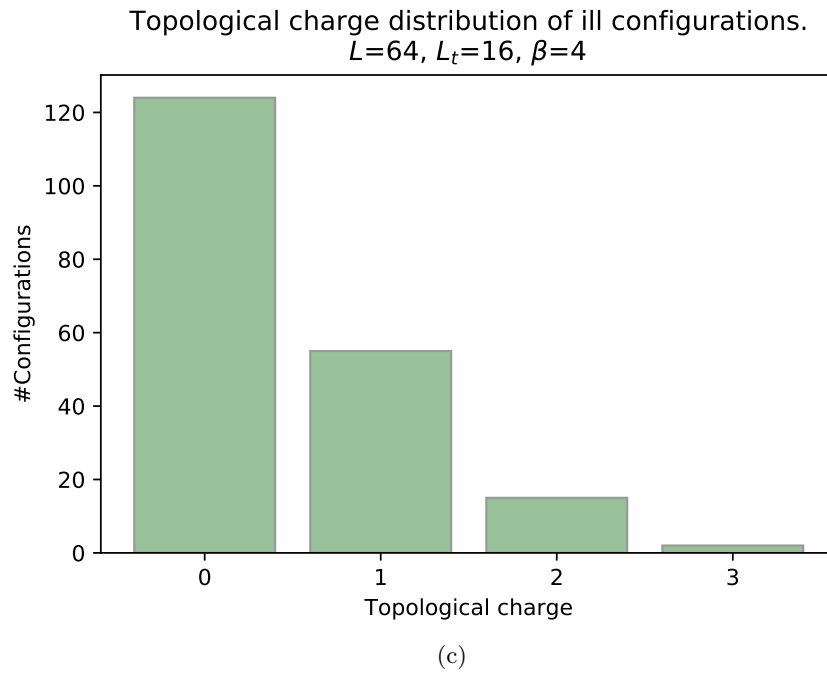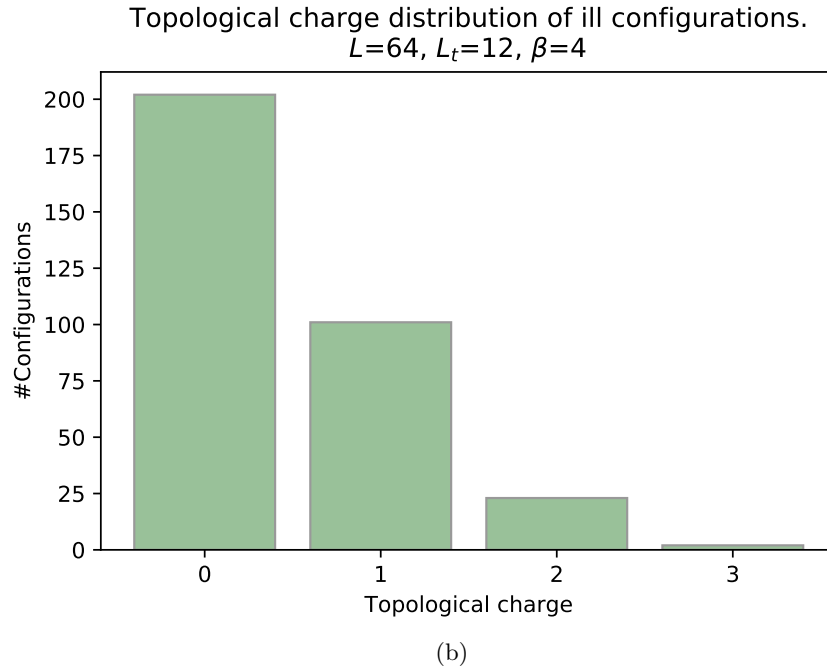Topological charge distribution of ill configurations.
$L=64$, $L_t=16$, $\beta=4$

(c)
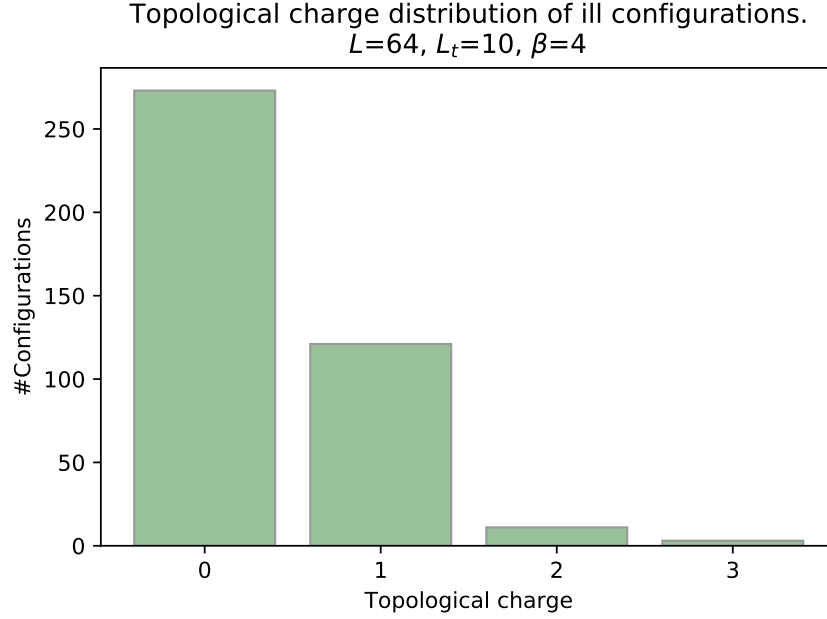
Figure 10: Topological charge distribution of the ill configurations